

Article

Detection and Analysis of Critical Dynamic Properties of Oligodendrocyte Differentiation

Svetoslav G. Nikolov ^{1,2,3,4,*} , Olaf Wolkenhauer ^{1,5} , Momchil Nenov ² and Julio Vera ⁴ 

- ¹ Department of Systems Biology and Bioinformatics, University of Rostock, 18051 Rostock, Germany
² Institute of Mechanics, Bulgarian Academy of Sciences, Acad. G. Bonchev Str., Bl. 4, 1113 Sofia, Bulgaria
³ Department of Mechanics, University of Transport, Geo Milev Str., 158, 1574 Sofia, Bulgaria
⁴ Laboratory of Systems Tumor Immunology, Department of Dermatology, University Hospital Erlangen, 91052 Erlangen, Germany
⁵ Stellenbosch Institute for Advanced Study (STIAS), Wallenberg Research Centre, Stellenbosch University, Stellenbosch 7600, South Africa
* Correspondence: s.nikolov@imbm.bas.bg; Tel.: +359-2-979-6411

Abstract: In this paper, we derive a four-dimensional ordinary differential equation (ODE) model representing the main interactions between Sox9, Sox10, Olig2 and several miRNAs, which drive the process of (oligo)dendrocyte differentiation. We utilize the Lyapunov–Andronov theory to analyze its dynamical properties. Our results indicated that the strength of external signaling (morphogenic gradients *shh* and *bmp*), and the transcription rate of mOlig2 explain the existence of stable and unstable (sustained oscillations) behavior in the system. Possible biological implications are discussed.

Keywords: oligodendrocytes; differentiation; mathematical model; stability; analysis

MSC: 34C23; 34C60; 92B05



Citation: Nikolov, S.G.; Wolkenhauer, O.; Nenov, M.; Vera, J. Detection and Analysis of Critical Dynamic Properties of Oligodendrocyte Differentiation.

Mathematics **2022**, *10*, 2928.

<https://doi.org/10.3390/math10162928>

Academic Editors: Irena Jadlovská, Tongxing Li, Syed Abbas and Said R Grace

Received: 6 July 2022

Accepted: 10 August 2022

Published: 14 August 2022

Publisher's Note: MDPI stays neutral with regard to jurisdictional claims in published maps and institutional affiliations.



Copyright: © 2022 by the authors. Licensee MDPI, Basel, Switzerland. This article is an open access article distributed under the terms and conditions of the Creative Commons Attribution (CC BY) license (<https://creativecommons.org/licenses/by/4.0/>).

1. Introduction

On a macroscopic level, the central nervous system (CNS) consists of gray and white matter. These terms reflect the visual appearance of the tissues, owing to the white color of myelin, a lipid rich substance that forms an interrupted insulating layer along the length of the axon—extensions of the neurons used to relay outgoing information over relatively long distances [1]. Gray matter is made up of the bodies of neurons, auxiliary cells called glia and unmyelinated neural fibers, whereas white matter consists of myelinated axons and glia cells responsible for their maintenance, including that of the myelin layer. In the CNS, the myelinating cells are called “oligodendrocytes”, reflecting their ability to form several myelin-filled protrusions, which wrap around adjacent axons.

The myelin layer is instrumental to the rapid propagation of neural signals [2], and damage to it results in reduced cognitive function. Diseases such as Multiple Sclerosis, which affect the myelin layer, are collectively known as “demyelinating diseases”. Since it is formed by oligodendrocytes, irregularities in oligodendrocyte function can be the root cause of demyelination.

During embryogenesis, oligodendrocytes (OLs) develop from progenitor cells called neural stem cells (NSC) in several loci and in several waves [3,4]. This differentiation process may have different stages, alternatives and end products, depending on its origin [3,5]. There are three different models describing the sequential stages in OL development reflecting this [6]. Proliferation-capable oligodendrocyte precursor cells (OPCs) exist in the adult vertebrate CNS, which can replenish dead OLs [7,8]. The differentiation program in OPCs is primed but suppressed through external signals [9]. Intercellular signaling guides both migration and differentiation [3]. A number of growth hormones (GFs),

transcription factors (TF) and non-coding RNAs have been implicated in the regulatory networks controlling OL differentiation [10–12] and myelination [13], making it possible to attempt to understand the underlying mechanisms as a system.

Several families of neural TFs and their mutual targets play a critical role in OL differentiation. Cantone and colleagues [14] utilized a bioinformatics and network biology analysis of transcriptomics and ChIP-Seq data from *in vivo* models of OL differentiation to systematically detect feedback and feedforward gene circuits driving OL differentiation. Their analysis delineated a complex regulatory architecture, in which central neural TFs such as Olig2, Sox10 and Tcf7l2 were upstream of and hierarchically regulated by other known TFs implicated in oligodendrogenesis such as Sox2, Sox6, Sox11, Nkx2-2, Nkx6-2, Hes5, Myt1 and Myrf. Interestingly, Olig2 and Sox10 established a tightly regulated, highly nonlinear gene subnetwork with several miRNAs, which contained feedback and feedforward loops upstream of multiple gene targets involved in the differentiation, migration and maturation of OLs [15]. Reiprich and coauthors [12] hypothesized that the dynamic regulation of this subnetwork through oligodendrogenesis may control an irreversible switch of cellular properties that contribute to terminal OL differentiation.

Another line of evidence suggests that spatiotemporal waves and oscillations in the activation of TF-driven gene circuits are essential to organizing cell differentiation and distribution in developing tissue. These circuits may operate as time-keepers, marking the rhythm of gene expression and tissue organization [16,17]. Tsiaris and colleagues [18] found that Notch-signaling-dependent synchronization of gene expression oscillations is necessary to re-establish the spatiotemporal patterns of gene expression required for proper tissue development. In the context of oligodendrogenesis, Sueda and Kageyama [19] combined observations made using time-lapsed imaging and immunohistological analyses of tissue and discovered that the expression of *Ascl1*, a TF involved in differentiation of brain cells, oscillated in proliferating OPCs; this occurred while this gene was repressed when OPCs differentiated into mature oligodendrocytes. Others have hypothesized that TF-expression oscillations maybe a mechanism for the fine-tuning and selection of gene targets that is triggered by certain stimulation scenarios [20].

As an interdisciplinary approach in the life sciences, systems biology aims to integrate experiments in iterative cycles with computational and mathematical modeling, simulations and theory [21]. The intersection between neurobiology and systems biology can be defined as systems neurobiology [22]. With the application of the systems neurobiological approach, it is possible to investigate essential properties of the central nervous system (CNS) [23].

The dynamic nature of intracellular regulatory systems, like those involved in OL differentiation, sometimes makes understanding cell behavior based solely on the association of expression profiles with phenotypes insufficient. Mathematical modeling OTOH can fill in the blanks between observable states with high infinite granularity.

For critical parameter values (also referred to as ‘bifurcation points’) the structures of the solutions in the mathematical models are essentially changed. In the neighborhood of bifurcation points, the dynamical behaviors of the biochemical system can change. As well, self-sustained oscillations can emerge/disappear from stable equilibria (steady states). Qualitatively, the appearance/disappearance of limited self-sustained oscillations corresponds to the so-called Andronov–Hopf bifurcation (AHb) [24,25]. AHb can be subcritical or supercritical. The nature of AHb is determined from the sign of the so-called first Lyapunov (focal) value, L_1 [26–28]. When L_1 is positive, then a hard (subcritical (un-reversible)) bifurcation takes place, as the (codimension-1) boundary of stability is ‘dangerous’ ([27,29,30]. In contrast, when L_1 is negative, then a soft (supercritical (reversible)) bifurcation occurs. The self-oscillations emerge as the system crosses the ‘safe’ boundary of stability. For instance, in [31], the analytical results (as Theorems) for stability and stability loss regarding the limit cycle in a high dimensional case (i.e., dimension $n \geq 3$) are shown.

Below, these analytical tools are used to investigate the reasons for the emergence of the different expression profiles of OLs.

2. Model

The model proposed in [14] describes the temporal variation in the expression of TFs, mRNAs and miRNAs in 14 ODEs, and is the starting point from which our model is derived. To facilitate both the exploration of the parameter space of the model and the interpretation of the results, this model was further simplified by categorizing all interactions into groups, and consolidating each group into one representative interaction. The reduced mathematical model (see Figure 1) of mSox9-mSox10-mOlig2-miR-17/335/338/155 regulatory circuit of the neural tube has the form

$$\begin{aligned}
 \dot{y}_1 &= k_1 + k_2 \frac{(I_1 + y_3^2 + y_1)^5}{(I_1 + y_3^2 + y_1)^5 + k_3^5} - k_4 y_1 - y_1 y_4, \\
 \dot{y}_2 &= k_8 \frac{I_2 + y_2}{I_2 + y_2 + k_9} - k_{10} y_2 - k_{11} y_2 y_4, \\
 \dot{y}_3 &= k_{15} \frac{(y_2 + y_3^2 + y_1)^2}{(y_2 + y_3^2 + y_1)^2 + k_{17}^2} - k_{18} y_3, \\
 \dot{y}_4 &= k_{22} \frac{y_3^2}{y_3^2 + k_{24}} - k_{23} y_4,
 \end{aligned}
 \tag{1}$$

where y_1 , y_2 and y_3 are three mRNAs (mOlig2, mSox9 and mSox10), and where y_4 represents the unification of four microRNAs (miR-17/335/338/155, respectively). According to [14] (Table S5 in Supplementary Materials), $k_7 = k_{BS}^{mSox9} = 0.004 \approx 0$; $k_{14} = k_{BS}^{mSox10} = 0.0015 \approx 0$; $k_{21} = k_{BS}^{miRNA} \approx 0$; $g_{Olig2} = 5.24 \approx 5$; $g_{Sox9} = 1.39 \approx 1$; $g_{Sox10} = 1.88 \approx 2$; $g_{mir338} = 0.9738 \approx 1$; $g_{mir335} = 0.87 \approx 1$; $g_{mir155} = 1$; $g_{mir17} = 0.99 \approx 1$; $g_{Tcf712} = 0.8 \approx 1$, and $g_{Myrf} = 1.46 \approx 1$. Here, we note that (i) in (1), the following substitutions are accepted: $ProtX_i = \alpha_i \cdot mRNA$, $\alpha_i = \frac{k_{s_i}}{k_{d_i}} \approx 1$ ($i = 1, 2, 3$); (ii) all model parameters are taken from [14] with dimension $[h^{-1}]$, and $input_{Shh} = I_1$ and $input_{BMPs} = I_2$ are antagonistic signals (morphogen gradients). The model (1) is considered to be a four-dimensional nonlinear dynamical system.

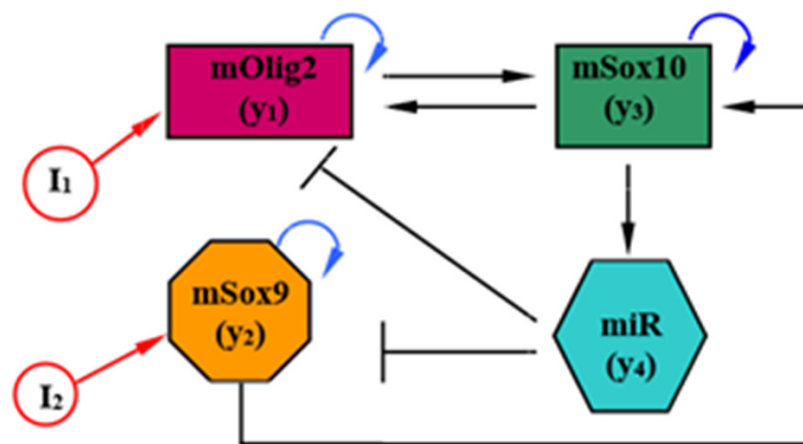


Figure 1. Scheme of the reduced model.

In a recent study of ours [32], the role of I_1 , I_2 and k_2 for the existence of stable and unstable (sustained oscillations) behaviors in system (1) was demonstrated through a numerical approach. Specifically, after direct numerical simulations, we ascertained that (i) for some relevant values of k_2 , I_1 and I_2 , system (1) is stable/unstable; (ii) depending on the values of k_2 , I_1 and I_2 , system (1) has one/two/three equilibria. Continuing with the study of this system, a new qualitative analysis of system (1) was performed according to the theory of Lyapunov–Andronov, and the new results can be cross-referenced using new numerical experiments (simulations).

3. Qualitative Analysis and Predictions

Let us consider system (2), which presents an autonomous nonlinear dynamical model. All constants of this model are real and positive.

Qualitative analysis of a dynamical system aims at revealing behavioral patterns that occur regardless of the adopted parameters [27,33]. Biological (biochemical) models are often subject to qualitative analysis, which can be a very useful approach to reveal complex dynamic behaviors.

Often, the qualitative analysis starts with the calculation of equilibrium (fixed) points. System (2) is multi-stationary and has several possible equilibria in the form

$$\begin{aligned}
 a_6\bar{y}_3^{12} + a_5\bar{y}_3^{10} + a_4\bar{y}_3^8 + a_3\bar{y}_3^6 + a_2\bar{y}_3^4 + a_1\bar{y}_3^2 + a_0 = 0, \quad \bar{y}_4 = \frac{k_{22}\bar{y}_3^2}{(\bar{y}_3^2 + k_{24})k_{23}}, \\
 \bar{y}_1^2 + 2\beta_1\bar{y}_1 + \gamma = 0, \quad \bar{y}_2^2 + \frac{\beta(k_9 + I_2) - k_8}{\beta}\bar{y}_2 - \frac{k_8 I_2}{\beta} = 0,
 \end{aligned}
 \tag{2}$$

where $a_0 - a_6$, β , β_1 and γ are coefficients (see Appendix A), and $k_1 - k_4$, $k_8 - k_{11}$, k_{15} , k_{17} , k_{18} , $k_{22} - k_{24}$ are parameters as in [14].

The equilibrium (fixed) points (2) of system (1) depend on a large number of parameters, which all have different ranges of variation; see Appendix A. After numerical calculations (for physiologically relevant values of $\bar{y}_1 \in [0, 1]$) of (1), we obtained that for (i) $I_1 = I_2 = 0$, system (1) had *one/two/three* real positive fixed points (equilibria); (ii) $I_1 = 0, I_2 \neq 0 (\in (0 - 0.6))$, system (1) had one equilibrium; (iii) $I_1 \neq 0, I_2 = 0$, system (1) had one equilibrium; and (iv) $I_1 \neq 0, I_2 \neq 0$, system (2) had one equilibrium. In the other words, the dynamic behavior of system (1) can be very different depending on the signals I_1 and I_2 . Note that stabilities, instabilities (including limit cycles (isolated periodic solutions)) and bistability all take place; see Figure A1 in Appendix C.

To check the qualitative features of system (1), we first exchanged the variables for local coordinates defined with respect to the fixed points (2), i.e., $y_i = \bar{y}_i + x_i, (i = 1 - 4)$. After that, we expanded the functional terms in (1) as a Maclaurin series (see Appendix A). Thus, the model (1) in local coordinates becomes

$$\begin{aligned}
 \frac{dx_1}{dt} &= \dot{x}_1 = c_1x_1 + c_2x_3 + c_3x_4 + c_4x_1^2 + c_5x_3^2 + c_6x_1x_3 - x_1x_4 + c_7x_1^3 + c_8x_3^3 + c_9x_1^2x_3 + c_{10}x_1x_3^2 + \dots h.o.t., \\
 \frac{dx_2}{dt} &= \dot{x}_2 = -c_{11}x_2 - c_{12}x_4 - c_{13}x_2^2 - k_{11}x_2x_4, \\
 \frac{dx_3}{dt} &= \dot{x}_3 = c_{14}x_1 + c_{14}x_2 + c_{15}x_3 + c_{16}x_1^2 + c_{16}x_2^2 + c_{17}x_3^2 + c_{18}x_1x_2 + c_{19}x_1x_3 + c_{19}x_2x_3 - c_{20}x_1^3 - \\
 &\quad - c_{20}x_2^3 + c_{21}x_3^3 - c_{22}x_1x_2^2 + c_{23}x_1x_3^2 + c_{23}x_2x_3^2 - c_{24}x_1^2x_2 - c_{25}x_1^2x_3 - c_{25}x_2^2x_3 - c_{26}x_1x_2x_3 + \dots h.o.t., \\
 \frac{dx_4}{dt} &= \dot{x}_4 = c_{27}x_3 - k_{23}x_4 + c_{28}x_3^2 - c_{29}x_3^3,
 \end{aligned}
 \tag{3}$$

where the analytical forms and numerical values of the coefficients for the equilibria and the original parameters are given in Appendix A. Hence, we find the Routh–Hurwitz stability conditions for (2) in the form

$$\begin{aligned}
 p &= k_{23} + c_{11} - c_1 - c_{15} > 0, \\
 q &= c_1(c_5 - c_{11} - k_{23}) + c_{11}(k_{23} - c_{15}) - c_2c_{14} - k_{23}c_{15} > 0, \\
 r &= -[k_{23}(c_1c_{11} - c_1c_{15} + c_2c_{14} + c_{11}c_{15}) + c_{11}(c_2c_{14} - c_1c_{15}) + c_{14}(c_3c_{27} - c_{12}c_{27})] > 0, \\
 s &= c_1(k_{23}c_{11}c_{15} - c_{12}c_{14}c_{27}) + c_{11}c_{14}(k_{23}c_2 + c_3c_{27}) > 0, \\
 R &= pqr - sp^2 - r^2 > 0.
 \end{aligned}
 \tag{4}$$

From here, our analysis focuses on the effects caused by changes in the bifurcation parameters k_2, I_1 and I_2 . According to [14] (Table S5 in Supplementary Materials), experimentally derived values for k_2 between 10% and 2 times the original value, i.e., $k_2 \in [0.04762, 0.95]$, are assumed. Since we do not know the exact values of some parameters of the model, we set $I_1 \in [0, 0.11]$ and $I_2 \in [0, 0.11]$, i.e., $I_1 + I_2 \in [0, 22]$. All other parameter values of system (1) were assigned according to [14] (Table S5 in Supplementary Materials) and are

$$\begin{aligned}
 k_1 &= 0.04719 [h^{-1}], k_3 = 0.4562 [h^{-1}], k_4 = 0.47619 [h^{-1}], k_8 = k_{10} = 0.0533 [h^{-1}], \\
 k_9 &= 0.4883 [h^{-1}], k_{11} = 0.4951 [h^{-1}], k_{15} = k_{18} = 0.1549 [h^{-1}], k_{17} = 0.6446 [h^{-1}], \\
 k_{22} &= 0.0274 [h^{-1}], k_{23} = 0.0289 [h^{-1}], k_{24} = 1.9098 [h^{-1}].
 \end{aligned}
 \tag{5}$$

To derive the analytic form (formula) of L_1 for model (3) (which is equivalent to (1)) we follow [26,27], as its numerical value (sign) is computed at bifurcation points, i.e., on the Andronov–Hopf boundary of stability $R = 0$. For more details, see Appendix B and Table 1. It is seen from Table 1 that the value (sign) of L_1 is positive for all computed bifurcation points, $(k_2^{bif}, I_1^{bif}, I_2^{bif})$, which indicated subcritical bifurcation. Therefore, the boundary of stability is dangerous and ‘hard’, meaning that irreversible loss of stability can occur. Note here that for the calculation of L_1 we use formula (A.11) because the sign of relation $4s - rp$ (see (5) or (A8)) at $R = 0$ is negative.

Table 1. Results for the first Lyapunov value (L_1), at different bifurcation values of parameters k_2, I_1, I_2 and different equilibrium states \bar{y}_4 .

I_1^{bif}, I_2^{bif}	k_2^{bif}	\bar{y}_4	L_1
0.05 0.05	0.1637	0.075	0.0154
0.05 0.05	0.1776	0.07	0.0507
0.1 0.1	0.0696	0.075	0.0517
0.1 0.1	0.0506	0.07	0.0789
0.11 0.11	0.068	0.08	0.0337

4. Numerical Investigation

Furthermore, we use numerical computations to determine the biological relevance of the analytical predictions obtained. For all numerical calculations, we have restricted ourselves to the variation of k_2, I_1 and I_2 . The other parameters remained same as (5).

First, we present a stable solution of system (1) when $I_1 = I_2 = 0$ and $k_2 = 0.4762$. As illustrated in Figure 2, this stable solution corresponded to a normal differentiation process of oligodendrocytes. In fact, according to the qualitative analysis of model (1), the latter had only one equilibrium. In passing, for $k_2 \in [0.04762, 0.95]$, there was no change in the dynamical behavior of system (1), i.e., we saw that changes of k_2 were not solely responsible for the occurrence of sustained periodic solutions of (1). We illustrated these results with the numerical example given in Figure A2 (see Appendix D). In Figure A2, the solutions for mOlig2 (y_1), miRNA (y_4), mSox9 (y_2) and mSox10 (y_3) were drawn for three different values of the parameter k_2 , i.e., $k_2 = 0.04762; 0.4762; 0.95$. The picture shows clearly how only the level of the solutions was different, whereas the behavior was similar.

In the framework of model (1), the values of k_2, I_1 and I_2 determined whether the system passed from a stable to an unstable state. In Figure 3, an unstable solution (sustained oscillation) of system (1) is shown at $k_2 = 0.085, I_1 = 0.1$ and $I_2 = 0.02$, i.e., $I_1 + I_2 = 0.12 = const$. System (1) was very close to the boundary of stability but was in the unstable zone.

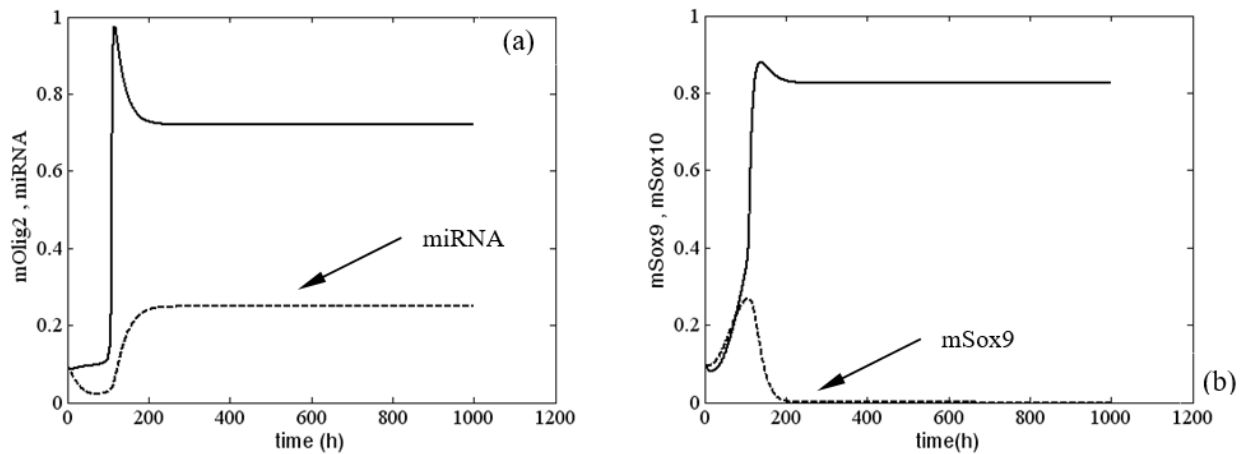


Figure 2. Time evolution of (a) $mOlig2(y_1)$, $miRNA(y_4)$; (b) $mSox9(y_2)$, $mSox10(y_3)$ at $k_2 = 0.4762$ and $I_1 = I_2 = 0$. Legend: (a) $mOlig2$ —solid line; (b) $mSox10$ —solid line. All other parameter values are as those in (5).

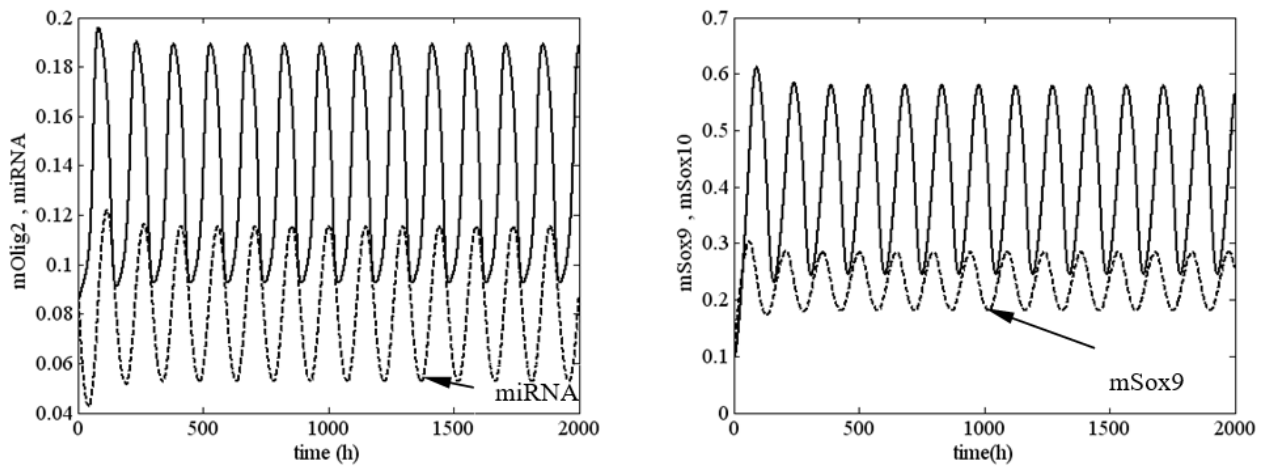


Figure 3. Sustained oscillations of system (1) at $k_2 = 0.085$, $I_1 = 0.1$ and $I_2 = 0.02$. Legend: $mOlig2$ —solid line (left panel); $mSox10$ —solid line (right panel). All other parameter values are as those in (5).

In Figure 4, we present a bifurcation diagram under variation of the control (bifurcation) parameters k_2 , I_1 and I_2 . The bifurcation diagram consists of two separate zones. They correspond to two coexisting behaviors and have been obtained using the same initial conditions, i.e., $y_1 = y_2 = y_3 = y_4 = 0.1$.

As one increases k_2 from 0.08 to 0.16, and I_1, I_2 from 0.01 to 0.11, the equilibrium (fixed) point becomes unstable at about $k_2 = 0.08$. When there is a subcritical Andronov–Hopf bifurcation (see Table 1), a limit cycle (sustained periodic oscillation) emerges, referred to as the period-1 limit cycle. From a dynamical point of view, this means we have a dangerous boundary of stability. In this case, when system (1) passes through this boundary, it escapes the old regime and runs away. Alternatively, the dangerous boundary can be divided into two subtypes [27,28,31]; (i) a *dynamically definite boundary*, where the transition process can be completed with stochastic character; and (ii) a *dynamically indefinite boundary* where the system has a limited number of periodic (limit cycles) solutions [34].

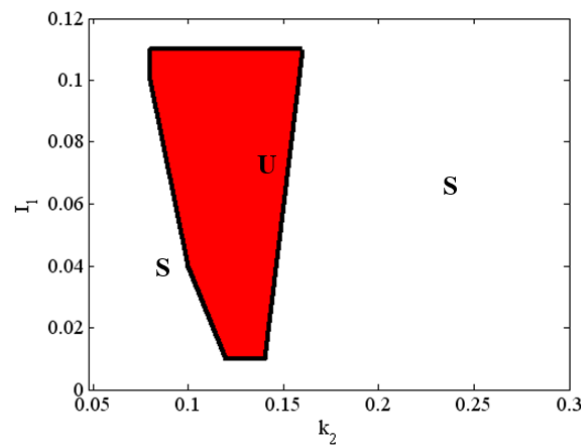


Figure 4. Bifurcation diagram of system (1) in the (I_1, k_2) space. Legend: U—unstable zone; S—stable zone; *solid line*—boundary of stability for Andronov–Hopf bifurcation. For clarity, the stable zone when $k_2 \in [0.3, 0.95]$ is not shown. All other parameter values are as those in (5), and $I_1 + I_2 = 0.12 = \text{const}$.

The results in Figures 3 and 4 require additional commentary from a dynamical point of view. A positive value of the first Lyapunov value corresponds to a ‘dangerous’ boundary of stability for the respective equilibrium state. This means that up until the moment of bifurcation in the phase space of the system, there exists an unstable limit cycle in the vicinity of the equilibrium point. If, at this point, the system is exposed to an external perturbation with an intensity higher than the amplitude of the limit cycle, the system will not return to its original equilibrium state but will instead adopt a different asymptotic behavior. This new behavior is fully deterministic but may be one of several possible behaviors. This is determined by the number of attractors, which affect the trajectory of the unstable limit cycle until it reaches the equilibrium state.

In Figure 5, we show the amplitude of the oscillations for different values of k_2 , I_1 and I_2 . The amplitude of mOlig2 oscillations gradually increases when the bifurcation parameter k_2 increases. On the other hand, if we compare the amplitude values from Figure 5a to Figure 5c, we can conclude that when the bifurcation parameters I_1 and I_2 increase (from 0.05 to 0.1, i.e., $I_1 + I_2$ increase), then the amplitude of oscillations decreases. Note that the maximal values of the oscillations also decrease. In general, the period of the oscillations is between 170 and 245 h, as it is the largest for $I_1 = I_2 = 0.01$; see Figure 6. In addition, for higher levels of k_2 (when $I_1 = I_2 = 0.01$) relaxant oscillations (slow-fast phases) for mOlig2 emerge; see Figure A3 in Appendix D.

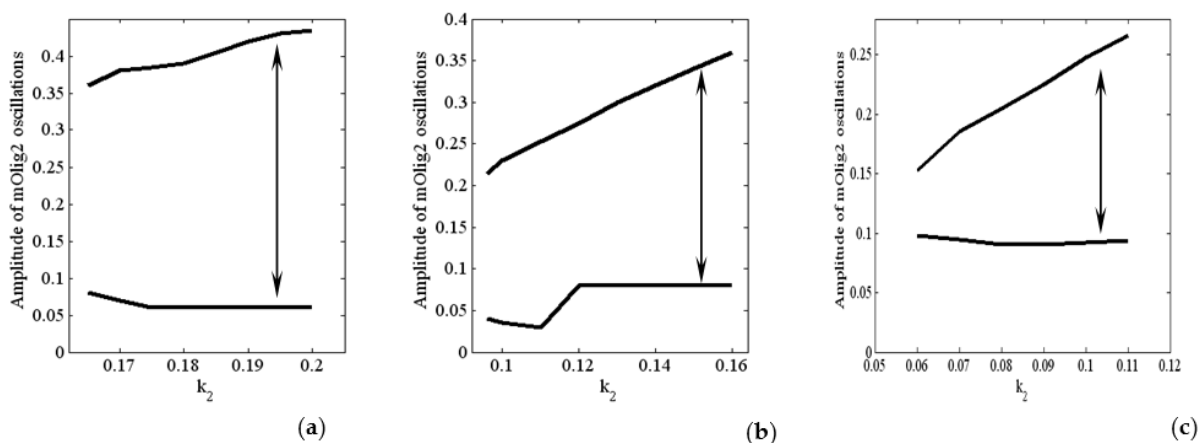


Figure 5. Amplitude of the oscillations as a function of the values of k_2 at: (a) $I_1 = I_2 = 0.01$; (b) $I_1 = I_2 = 0.05$; (c) $I_1 = I_2 = 0.1$. All other parameter values are as those in (5).

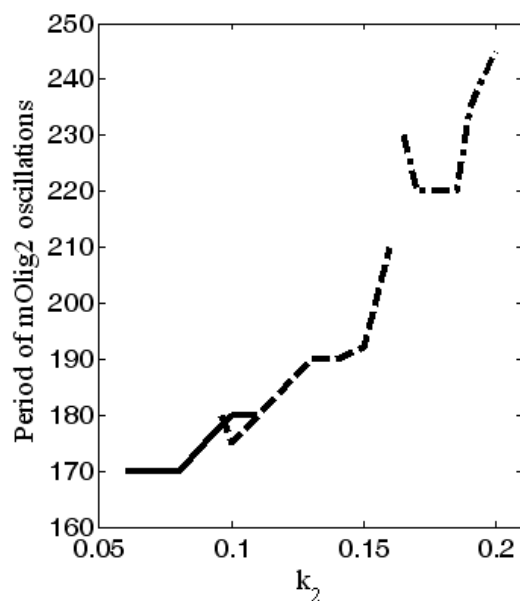


Figure 6. Dependence of period of oscillations on the values of k_2 at $I_1 = I_2 = 0.01$ —dash dot line; $I_1 = I_2 = 0.05$ —dashed line; $I_1 = I_2 = 0.1$ —solid line. All other parameter values are as those in (5).

In Figure 6, the range of the period of oscillations of Olig2 is ~ 1.5 to 2.5 times the duration of differentiation proper (4 days) [35]. A differentiating OPC would therefore experience levels of Olig2 determined by a single slope, peak or dip. However, OPCs stuck in the proliferation phase may experience multiple oscillations. Without the external signals from the morphogenic gradients *shh* (I_1) and *bmp* (I_2), the expression levels of the major TFs are stable (see Figure 2). As the cell travels along the gradient, there is a potential critical point, determined by a combination of signal strength I_i ($i = 1, 2$) and sensitivity k_2 (see Figure 4 red area), where they start to oscillate (see Figure 3). This will result in different expression profiles depending on their position on the TF concentration curve. A new, stable equilibrium may emerge if noise exceeds the amplitude of the signal. If that happens with statistical regularity, it will result in a specific distribution of outcomes, i.e., phenotypes.

5. Discussion and Conclusions

A large number of the phenomena in nature and technology have a dynamic character, owing to their non-linearity. The discipline responsible for research into dynamic processes is called non-linear dynamics. Its purpose is to find out the laws governing non-linear dynamic processes. Since the time of Sir Isaac Newton, the approach to researching a phenomenon has been to first make observations based on experiments, and then to construct a mathematical model described by differential equations (ODE, PDE, DDE etc.) and analyze it. Finally, the results from the model are compared to the prototype. In non-linear dynamics, mathematical models are represented through systems of equations with analytically chosen non-linearity, and a finite number of parameters. It is worth noting that most models in non-linear dynamics cannot be exhaustively analyzed. Instead, qualitative analysis (bifurcation theory) of the dynamic systems can be used to explain and predict the appearance or disappearance of states and movements. In this article, we explored a mathematical model consisting of four non-linear ODEs describing the temporal variation in the expression of transcription factors and micro RNAs that drive the differentiation process of oligodendrocytes using a special version of the quality theory of ODEs: Lyapunov–Andronov bifurcation theory.

Based upon our results, a number of different outcomes for the differentiating cell are possible:

Case A: The cell does not pass through the red zone in Figure 4 (determined by the strength of the morphogenic signal $I_i (i = 1, 2)$ and the sensitivity k_2); no bifurcation occurs, and TF levels remain stable.

Case B: The cell passes through the red zone but spends a physiologically insignificant amount of time in an unstable state due to noise, jumping to a different TF concentration equilibrium than the original value.

Case C: The system remains in an unstable state long enough to experience an oscillating signal. However, the noise level does not become high enough to push it out of the boundary cycle.

Case D: A statistically determined percentage of cells fall into either category B or C, or anywhere in between, resulting in several different phenotypes without the need for added complexity.

Finally, we note that (1) all our speculations and predictions from a biological point of view need experimental confirmation in the form of dynamic data for TF concentrations; (2) from a mathematical point of view, a possible future consideration is the investigation of model (1) in a fractional sense.

Author Contributions: The initial idea for investigation comes from S.G.N. and J.V. The model was computed and simulated by all co-authors. Qualitative analysis was performed by S.G.N. The manuscript was drafted by all co-authors. All authors have read and agreed to the published version of the manuscript.

Funding: Author Svetoslav G. Nikolov wishes to acknowledge partial support for this work from the Bulgarian National Science Fund (Grant KII-06-H57/18).

Institutional Review Board Statement: Not applicable.

Informed Consent Statement: Not applicable.

Data Availability Statement: Not applicable.

Conflicts of Interest: The authors declare no conflict of interest.

Appendix A. Qualitative Analysis: Fixed Points (Equilibrium States) Derivation

The equilibria of the model (1) are calculated using the following equations:

$$a_6 \bar{y}_3^{12} + a_5 \bar{y}_3^{10} + a_4 \bar{y}_3^8 + a_3 \bar{y}_3^6 + a_2 \bar{y}_3^4 + a_1 \bar{y}_3^2 + a_0 = 0, \quad \bar{y}_4 = \frac{k_{22} \bar{y}_3^2}{(\bar{y}_3^2 + k_{24}) k_{23}}, \quad (A1)$$

$$\bar{y}_1^2 + 2\beta_1 \bar{y}_1 + \gamma = 0, \quad \bar{y}_2^2 + \frac{\beta(k_9 + I_2) - k_8}{\beta} \bar{y}_2 - \frac{k_8 I_2}{\beta} = 0,$$

where

$$k_1 = k_{BSmOlig2}, k_2 = k_{tranmOlig2}, k_3 = k_{mOlig2}, k_4 = k_{degmOlig2}, k_8 = k_{tranmSox9}, k_9 = k_{mSox9}, k_{11} = k_{inhmSox9}, k_{17} = k_{mSox10}, k_{24} = k_{mmir338}, a_6 = k_1 + k_2 - A, k_{10} = k_{degmSox9}, k_{15} = k_{tranmSox10}, k_{18} = k_{degmSox10}, k_{22} = k_{tranmiR338}, k_{23} = k_{degmiR338}, a_5 = (k_1 + k_2)(5\alpha + k_{24}) - 5A\alpha - B, a_4 = 5\alpha[(k_1 + k_2)(2\alpha + k_{24}) - B - 2A\alpha], a_3 = 10\alpha^2[(k_1 + k_2)(\alpha + k_{24}) - A\alpha - B], a_2 = 5\alpha^3[(k_1 + k_2)(2k_{24} + \alpha) - A\alpha - 2B], a_1 = k_1(5k_{24} + \alpha^5 + k_{35}) + k_2\alpha^4(5k_{24} + \alpha) - Ak_{35} - 5\alpha^4B - A\alpha^5, a_0 = k_1k_{24}(k_{35} + \alpha^5) + k_2k_{24}\alpha^5 - B(k_{35} + \alpha^5), \alpha = I_1 + y_1, A = y_1(1 + k_4), B = y_1k_4k_{24}, \beta = k_8 + k_{11}y_4, \beta_1 = y_2 + y_3^2, \gamma = \beta_{12} - k_{17}k_{18}y_3k_{15} - k_{18}y_3. \quad (A2)$$

To investigate the type of (A1), it is supposed that

$$y_i = \bar{y}_i + x_i \quad (i = 1 - 4). \quad (A3)$$

To determine analytically the character of (A1), we transform system (1)

The functions $\frac{1}{\varepsilon_i + \psi_i}$ in Maclaurin series have the form

$$\frac{1}{\varepsilon_i + \psi_i} = \frac{1}{\varepsilon_i \left(1 + \frac{\psi_i}{\varepsilon_i}\right)} = \frac{1}{\varepsilon_i} \left[1 - \frac{\psi_i}{\varepsilon_i} + \left(\frac{\psi_i}{\varepsilon_i}\right)^2 - \left(\frac{\psi_i}{\varepsilon_i}\right)^3 + \dots\right], \tag{A4}$$

where

$$\begin{aligned} \varepsilon_1 &= k_3^5, \varepsilon_2 = k_9, \varepsilon_3 = k_{17}^2, \varepsilon_4 = k_{24}, \psi_1 = \left[I_1 + (\bar{y}_3 + x_3)^2 + \bar{y}_1 + x_1\right]^5, \\ \psi_2 &= I_2 + \bar{y}_2 + x_2, \psi_3 = \left[\bar{y}_2 + x_2 + (\bar{y}_3 + x_3)^2 + \bar{y}_1 + x_1\right]^2, \psi_4 = (\bar{y}_3 + x_3)^2. \end{aligned} \tag{A5}$$

If we restrict ourselves to the linear terms from (A4), then after substitution of (A4) and (A3) into (1), (1) takes the form

$$\begin{aligned} \frac{dx_1}{dt} &= \dot{x}_1 = c_1x_1 + c_2x_3 + c_3x_4 + c_4x_1^2 + c_5x_3^2 + c_6x_1x_3 - x_1x_4 + c_7x_1^3 + c_8x_3^3 + c_9x_1^2x_3 + c_{10}x_1x_3^2 + \dots \text{h.o.t.}, \\ \frac{dx_2}{dt} &= \dot{x}_2 = -c_{11}x_2 - c_{12}x_4 - c_{13}x_2^2 - k_{11}x_2x_4, \\ \frac{dx_3}{dt} &= \dot{x}_3 = c_{14}x_1 + c_{14}x_2 + c_{15}x_3 + c_{16}x_1^2 + c_{16}x_2^2 + c_{17}x_3^2 + c_{18}x_1x_2 + c_{19}x_1x_3 + c_{19}x_2x_3 - c_{20}x_1^3 - \\ &\quad - c_{20}x_2^3 + c_{21}x_3^3 - c_{22}x_1x_2^2 + c_{23}x_1x_3^2 + c_{23}x_2x_3^2 - c_{24}x_1^2x_2 - c_{25}x_1^2x_3 - c_{25}x_2^2x_3 - c_{26}x_1x_2x_3 + \dots \text{h.o.t.}, \\ \frac{dx_4}{dt} &= \dot{x}_4 = c_{27}x_3 - k_{23}x_4 + c_{28}x_3^2 - c_{29}x_3^3, \end{aligned} \tag{A6}$$

where

$$\begin{aligned} c_1 &= -k_4 - \bar{y}_4 + \frac{k_2\rho_1}{\varepsilon_1} \left(1 - \frac{2\rho_0}{\varepsilon_1}\right), c_2 = \frac{k_2\rho_2}{\varepsilon_1} \left(1 - \frac{2\rho_0}{\varepsilon_1}\right), c_3 = -\bar{y}_1, c_4 = \frac{k_2}{\varepsilon_1} \left(\rho_3 - \frac{2\rho_0\rho_3 + \rho_1^2}{\varepsilon_1}\right), \\ c_5 &= \frac{k_2}{\varepsilon_1} \left(\rho_4 - \frac{2\rho_0\rho_4 + \rho_2^2}{\varepsilon_1}\right), c_6 = \frac{k_2}{\varepsilon_1} \left(\rho_5 - \frac{2(\rho_1\rho_2 + \rho_0\rho_5)}{\varepsilon_1}\right), c_7 = \frac{k_2}{\varepsilon_1} \left(\rho_6 - \frac{2(\rho_0\rho_6 + \rho_1\rho_3)}{\varepsilon_1}\right), \\ c_8 &= \frac{k_2}{\varepsilon_1} \left(\rho_7 - \frac{2(\rho_0\rho_7 + \rho_2\rho_4)}{\varepsilon_1}\right), c_9 = \frac{k_2}{\varepsilon_1} \left(\rho_8 - \frac{2(\rho_1\rho_5 + \rho_2\rho_3 + \rho_0\rho_8)}{\varepsilon_1}\right), \\ c_{10} &= \frac{k_2}{\varepsilon_1} \left(\rho_9 - \frac{2(\rho_2\rho_5 + \rho_1\rho_4 + \rho_0\rho_9)}{\varepsilon_1}\right), c_{11} = k_{10} + k_{11}\bar{y}_4 + \frac{k_8}{\varepsilon_2^2} [\varepsilon_2 - 2(I_2 + \bar{y}_2)], \\ c_{12} &= k_{11}\bar{y}_2, c_{13} = \frac{k_8}{\varepsilon_2^2}, c_{14} = \frac{2k_{15}\theta_0}{\varepsilon_3^2} (\varepsilon_3 - 2\theta_0^2), c_{15} = \frac{2k_{15}\theta_0\theta_1}{\varepsilon_3^2} (\varepsilon_3 - 2\theta_0^2) - k_{18}, c_{16} = \frac{k_{15}}{\varepsilon_3^2} (\varepsilon_3 - 6\theta_0^2), \\ c_{17} &= \frac{k_{15}}{\varepsilon_3^2} [\varepsilon_3(2\theta_0 + \theta_1^2) - 2\theta_0^2(2\theta_0 + 3\theta_1^2)], c_{18} = \frac{2k_{15}}{\varepsilon_3^2} (\varepsilon_3 - 6\theta_0^2), c_{19} = \frac{2k_{15}\theta_1}{\varepsilon_3^2} (\varepsilon_3 - 6\theta_0^2), \\ c_{20} &= \frac{4k_{15}\theta_0}{\varepsilon_3^3}, c_{21} = \frac{2k_{15}\theta_1}{\varepsilon_3^2} (\varepsilon_3 - 6\theta_0^2 - 2\theta_0\theta_1^2), c_{22} = \frac{12k_{15}\theta_0}{\varepsilon_3^3}, c_{23} = \frac{2k_{15}}{\varepsilon_3^2} [\varepsilon_3 - 6\theta_0(\theta_0 + \theta_1^2)], \\ c_{24} &= -\frac{12k_{15}\theta_0}{\varepsilon_3^3}, c_{25} = -\frac{12k_{15}\theta_0\theta_1}{\varepsilon_3^3}, c_{26} = -\frac{24k_{15}\theta_0\theta_1}{\varepsilon_3^3}, c_{27} = \frac{2k_{22}\bar{y}_3}{\varepsilon_4^2} (\varepsilon_4 - 2\bar{y}_3^2), \\ c_{28} &= \frac{k_{22}}{\varepsilon_4^2} (\varepsilon_4 - 6\bar{y}_3^2), c_{29} = \frac{4k_{22}\bar{y}_3}{\varepsilon_4^2}, \theta_0 = \bar{y}_1 + \bar{y}_2 + \bar{y}_3^2, \theta_1 = 2\bar{y}_3, \zeta = I_1 + \bar{y}_1, \\ \rho_0 &= \zeta^5 + 5\zeta^4\bar{y}_3^2 + 10\zeta^3\bar{y}_3^4 + 10\zeta^2\bar{y}_3^6 + 5\zeta\bar{y}_3^8 + \bar{y}_3^{10}, \rho_1 = 5\zeta^4 + 20\zeta^3\bar{y}_3^2 + 30\zeta^2\bar{y}_3^4 + 20\zeta\bar{y}_3^6 + 5\bar{y}_3^8, \\ \rho_2 &= 10\zeta^4\bar{y}_3 + 40\zeta^3\bar{y}_3^3 + 60\zeta^2\bar{y}_3^5 + 40\zeta\bar{y}_3^7 + 10\bar{y}_3^9, \rho_3 = 10\zeta^3 + 30\zeta^2\bar{y}_3^2 + 30\zeta\bar{y}_3^4 + 10\bar{y}_3^6, \\ \rho_4 &= 5\zeta^4 + 60\zeta^3\bar{y}_3^2 + 150\zeta^2\bar{y}_3^4 + 140\zeta\bar{y}_3^6 + 45\bar{y}_3^8, \rho_5 = 40(\zeta^3\bar{y}_3 + 3\zeta^2\bar{y}_3^3 + 3\zeta\bar{y}_3^5 + \bar{y}_3^7), \\ \rho_6 &= 10(\zeta^2 + 2\zeta\bar{y}_3^2 + \bar{y}_3^4), \rho_7 = 10(4\zeta^3\bar{y}_3 + 20\zeta^2\bar{y}_3^3 + 9\zeta\bar{y}_3^5 + 12\bar{y}_3^7), \rho_8 = 60(\zeta^2\bar{y}_3 + 2\zeta\bar{y}_3^3 + \bar{y}_3^5), \\ \rho_9 &= 20(\zeta^3 + 9\zeta^2\bar{y}_3^2 + 15\zeta\bar{y}_3^4 + 7\bar{y}_3^6). \end{aligned} \tag{A7}$$

For (A1), the Routh–Hurwitz conditions for stability become

$$\begin{aligned} p &= k_{23} + c_{11} - c_1 - c_{15} > 0, \\ q &= c_1(c_{15} - c_{11} - k_{23}) + c_{11}(k_{23} - c_{15}) - c_2c_{14} - k_{23}c_{15} > 0, \\ r &= -[k_{23}(c_1c_{11} - c_1c_{15} + c_2c_{14} + c_{11}c_{15}) + c_{11}(c_2c_{14} - c_1c_{15}) + c_{14}(c_3c_{27} - c_{12}c_{27})] > 0, \\ s &= c_1(k_{23}c_{11}c_{15} - c_{12}c_{14}c_{27}) + c_{11}c_{14}(k_{23}c_2 + c_3c_{27}) > 0, \\ R &= pqr - sp^2 - r^2 > 0. \end{aligned} \tag{A8}$$

In (A8), the notations p, q, r, s and R are as those in [26]. In four dimensional systems, it is argued that the boundaries of stability are $s = 0$ and $R = 0$, so that we are interested whether s and R are negative when the conditions p, q and r are always positive. For $s = 0$, the characteristic equation has one zero root, and $R = 0$ has a pair of pure imaginary roots.

The type of stability loss (crossing boundary $R = 0$) depends on the sign of first Lyapunov value L_1 .

Appendix B. Calculation of L_1

For dynamical systems, the first Lyapunov value is a well-established tool for making qualitative predictions about the long-term behavior of the system. To explain this, following [26], we calculate L_1 (for detailed discussion of L_1 , see appendix in [36] or also [27,28,37–42]) close to the boundary of stability $R = 0$ of system (1). According to the Andronov–Hopf theory, the following relations are valid: (i) the sign of L_1 (at $R = 0$) defines the type (stable or instable) of equilibrium state; (ii) the type of equilibrium state (at $R = 0$) qualitatively defines the reconstruction of phase space. For four first-order nonlinear differential equations, there exists a strong connection between the analytical form of first Lyapunov value, and the sign of relation $4s - rp$ (see (A8)) at $R = 0$:

case A. $4s - rp > 0$ —the characteristic equation has only complex roots

$$\begin{aligned}
 L_1 = & \frac{\pi}{4b^2} \left\{ 2 \left(A_{22}^{(1)} A_{22}^{(2)} - A_{11}^{(1)} A_{11}^{(2)} \right) - 2A_{12}^{(2)} \left(A_{11}^{(2)} + A_{22}^{(2)} \right) + 2A_{12}^{(1)} \left(A_{11}^{(1)} + A_{22}^{(1)} \right) + 3b \left(A_{111}^{(1)} + A_{222}^{(2)} + A_{112}^{(2)} + A_{122}^{(1)} \right) + \right. \\
 & + \frac{2b}{\Delta} \left[2 \left(A_{23}^{(1)} + A_{13}^{(2)} \right) \Delta_3 \left[-b\Delta_2 A_{11}^{(3)} + m\Delta_1 A_{12}^{(3)} + b\Delta_2 A_{22}^{(3)} - 2bmnA_{11}^{(4)} + n\Delta_4 A_{12}^{(4)} + 2bmnA_{22}^{(4)} \right] + \right. \\
 & + 2 \left(A_{24}^{(1)} + A_{14}^{(2)} \right) \Delta_3 \left[-n\Delta_4 A_{12}^{(3)} + m\Delta_1 A_{12}^{(4)} - b\Delta_2 A_{11}^{(4)} - 2bmnA_{22}^{(3)} + b\Delta_2 A_{22}^{(4)} + 2bmnA_{11}^{(3)} \right] + \\
 & + \left(3A_{13}^{(1)} + A_{23}^{(2)} \right) \left[m\Delta_3^2 A_{11}^{(3)} + 2b^2 m\Delta_5 A_{11}^{(3)} + 2b\Delta_2 \Delta_3 A_{12}^{(3)} - 2b^2 m\Delta_6 A_{22}^{(3)} + n\Delta_3^2 A_{11}^{(4)} - 2b^2 n\Delta_6 A_{11}^{(4)} + \right. \\
 & + 4mnb\Delta_3 A_{12}^{(4)} + 2b^2 n\Delta_5 A_{22}^{(4)} \left. \right] + \left(3A_{14}^{(1)} + A_{24}^{(2)} \right) \left[2b^2 n\Delta_6 A_{11}^{(3)} - n\Delta_3^2 A_{11}^{(3)} - 4mnb\Delta_3 A_{12}^{(3)} - 2b^2 n\Delta_5 A_{22}^{(3)} + \right. \\
 & + m\Delta_3 \Delta_7 A_{11}^{(4)} + 8mb^2 \left(b^2 - n^2 \right) A_{11}^{(4)} + 2b\Delta_2 \Delta_3 A_{12}^{(4)} - 2b^2 m\Delta_6 A_{22}^{(4)} \left. \right] + \left(3A_{23}^{(2)} + A_{13}^{(1)} \right) \left[-2b^2 m\Delta_6 A_{11}^{(3)} - \right. \\
 & - 2b\Delta_2 \Delta_3 A_{12}^{(3)} + 2b^2 m\Delta_5 A_{22}^{(3)} + m\Delta_3^2 A_{22}^{(3)} + 2b^2 n\Delta_5 A_{11}^{(4)} - 4bmn\Delta_3 A_{12}^{(4)} - 2nb^2 \Delta_6 A_{22}^{(4)} + n\Delta_3 A_{22}^{(4)} \left. \right] + \\
 & + \left(3A_{24}^{(2)} + A_{14}^{(1)} \right) \left[4bmn\Delta_3 A_{12}^{(3)} - 2b^2 n\Delta_5 A_{11}^{(3)} - n\Delta_3^2 A_{22}^{(3)} + 2b^2 n\Delta_6 A_{22}^{(3)} - 2b^2 m\Delta_6 A_{11}^{(4)} - 2b\Delta_2 \Delta_3 A_{12}^{(4)} + \right. \\
 & \left. \left. + m\Delta_3^2 A_{22}^{(4)} + 2b^2 m\Delta_5 A_{22}^{(4)} \right] \right\}, \tag{A9}
 \end{aligned}$$

where

$$\begin{aligned}
 \Delta_1 &= m^2 + n^2 + 4b^2, \quad \Delta_2 = m^2 - n^2 + 4b^2, \quad \Delta_3 = m^2 + n^2, \\
 \Delta_4 &= m^2 + n^2 - 4b^2, \quad \Delta_5 = 4b^2 + 3m^2 - n^2, \quad \Delta_6 = 3n^2 - m^2 - 4b^2, \\
 \Delta_7 &= m^2 + n^2 + 6b^2, \quad b^2 = \frac{r}{p}, \quad m = -\frac{p}{2}, \quad n^2 = \frac{sp}{r} - \frac{p^2}{4} \text{ or } n^2 = \frac{p^2}{4} - \frac{sp}{r}. \tag{A10}
 \end{aligned}$$

case B. $4s - rp < 0$ —the characteristic equation has both real and complex roots:

$$\begin{aligned}
 L_1 = & \frac{\pi}{4b^2} \left\{ 2 \left(A_{22}^{(1)} A_{22}^{(2)} - A_{11}^{(1)} A_{11}^{(2)} \right) - 2 \left(A_{11}^{(2)} + A_{22}^{(2)} \right) A_{12}^{(2)} + 2 \left(A_{11}^{(1)} + A_{22}^{(1)} \right) A_{12}^{(1)} + 3b \left(A_{111}^{(1)} + A_{222}^{(2)} + A_{112}^{(2)} + A_{122}^{(1)} \right) + \right. \\
 & + \frac{2b}{m(m^2 + 4b^2)} \left[2m \left(A_{23}^{(1)} + A_{13}^{(2)} \right) \left(bA_{11}^{(3)} - bA_{22}^{(3)} - mA_{12}^{(3)} \right) - \left(m^2 + 8b^2 \right) \left(A_{11}^{(3)} A_{23}^{(2)} + A_{22}^{(3)} A_{13}^{(1)} \right) + \right. \\
 & + 4mb \left(A_{12}^{(3)} A_{23}^{(2)} - A_{13}^{(1)} A_{12}^{(3)} \right) - \left(3m^2 + 8b^2 \right) \left(A_{11}^{(3)} A_{13}^{(1)} + A_{22}^{(3)} A_{23}^{(2)} \right) \left. \right] + \frac{2b}{n(n^2 + 4b^2)} \left[2n \left(A_{24}^{(1)} + A_{14}^{(2)} \right) \times \right. \\
 & \times \left(bA_{11}^{(4)} - bA_{22}^{(4)} - nA_{12}^{(4)} \right) - \left(n^2 + 8b^2 \right) \left(A_{11}^{(4)} A_{24}^{(2)} + A_{22}^{(4)} A_{14}^{(1)} \right) + 4nb \left(A_{12}^{(4)} A_{24}^{(2)} - A_{14}^{(1)} A_{12}^{(4)} \right) - \\
 & \left. \left. - \left(3n^2 + 8b^2 \right) \left(A_{11}^{(4)} A_{14}^{(1)} + A_{22}^{(4)} A_{24}^{(2)} \right) \right] \right\}. \tag{A11}
 \end{aligned}$$

We note that corresponding formulas and definitions of the coefficients $A_{ij}^{(l)}$ and $A_{ijk}^{(l)}$ ($i, j, k, l = 1, 2, 3, 4$) can be seen in [26]. For system (A.6), we need to perform an extra study. The complete elaboration of $A_{ij}^{(l)}$ and $A_{ijk}^{(l)}$ is

$$\begin{aligned}
 A_{11}^{(l)} &= \frac{1}{\Delta_0} \{ \alpha'_{11} [c_4 \alpha_{11}^2 + c_5 \alpha_{31}^2 + 2\alpha_{11}(c_6 \alpha_{31} - \alpha_{41})] - \alpha'_{12} \alpha_{21} (c_{13} \alpha_{21} + 2k_{11} \alpha_{41}) + \\
 &\quad + \alpha'_{13} [c_{16} (\alpha_{11}^2 + \alpha_{21}^2) + c_{17} \alpha_{31}^2 + 2\alpha_{11}(c_{18} \alpha_{21} + c_{19} \alpha_{31}) + 2c_{19} \alpha_{21} \alpha_{31}] + \alpha'_{14} c_{28} \alpha_{31}^2 \}, \\
 A_{12}^{(l)} &= \frac{1}{\Delta_0} \{ \alpha'_{11} [c_4 \alpha_{11} \alpha_{12} + c_5 \alpha_{31} \alpha_{32} + c_6 (\alpha_{11} \alpha_{32} + \alpha_{12} \alpha_{31})] - \alpha'_{12} [c_{13} \alpha_{21} \alpha_{22} + k_{11} (\alpha_{21} \alpha_{42} + \alpha_{22} \alpha_{41})] + \\
 &\quad + \alpha'_{13} [c_{16} (\alpha_{11} \alpha_{12} + \alpha_{21} \alpha_{22}) + c_{17} \alpha_{31} \alpha_{32} + c_{18} (\alpha_{11} \alpha_{22} + \alpha_{12} \alpha_{21}) + c_{19} (\alpha_{11} \alpha_{32} + \alpha_{12} \alpha_{31}) + \\
 &\quad + c_{19} (\alpha_{21} \alpha_{32} + \alpha_{22} \alpha_{31})] + \alpha'_{14} c_{28} \alpha_{31} \alpha_{32} \}, \\
 A_{22}^{(l)} &= \frac{1}{\Delta_0} \{ \alpha'_{11} (c_4 \alpha_{12}^2 + c_5 \alpha_{32}^2 + 2c_6 \alpha_{12} \alpha_{32} - 2\alpha_{12} \alpha_{42}) - \alpha'_{12} \alpha_{22} (c_{13} \alpha_{22} + 2k_{11} \alpha_{42}) + \\
 &\quad + \alpha'_{13} [c_{16} (\alpha_{11}^2 + \alpha_{22}^2) + c_{17} \alpha_{32}^2 + 2\alpha_{12} (c_{18} \alpha_{22} + c_{19} \alpha_{32}) + 2c_{19} \alpha_{22} \alpha_{32}] + \alpha'_{14} c_{28} \alpha_{32}^2 \}, \\
 A_{13}^{(l)} &= \frac{1}{\Delta_0} \{ \alpha'_{11} [c_4 \alpha_{11} \alpha_{13} + c_5 \alpha_{31} \alpha_{33} + c_6 (\alpha_{11} \alpha_{33} + \alpha_{13} \alpha_{31}) - \alpha_{11} \alpha_{43} - \alpha_{13} \alpha_{41}] - \\
 &\quad - \alpha'_{12} [c_{13} \alpha_{21} \alpha_{23} + k_{11} (\alpha_{21} \alpha_{43} + \alpha_{23} \alpha_{41})] + \alpha'_{13} [c_{16} (\alpha_{11} \alpha_{13} + \alpha_{21} \alpha_{23}) + c_{17} \alpha_{31} \alpha_{33} + c_{18} (\alpha_{11} \alpha_{23} + \alpha_{13} \alpha_{21}) + \\
 &\quad + c_{19} (\alpha_{11} \alpha_{33} + \alpha_{13} \alpha_{31}) + c_{19} (\alpha_{21} \alpha_{33} + \alpha_{23} \alpha_{31}) + \alpha'_{14} c_{28} \alpha_{31} \alpha_{33} \}, \\
 A_{14}^{(l)} &= \frac{1}{\Delta_0} \{ \alpha'_{11} [c_4 \alpha_{11} \alpha_{14} + c_5 \alpha_{31} \alpha_{34} + c_6 (\alpha_{11} \alpha_{34} + \alpha_{14} \alpha_{31}) - \alpha_{11} \alpha_{44} + \alpha_{14} \alpha_{41}] - \alpha'_{12} k_{11} \alpha_{21} \alpha_{44} + \\
 &\quad + \alpha'_{13} [c_{16} \alpha_{11} \alpha_{14} + c_{17} \alpha_{31} \alpha_{34} + c_{18} \alpha_{14} \alpha_{21} + c_{19} (\alpha_{11} \alpha_{34} + \alpha_{14} \alpha_{31}) + c_{19} \alpha_{21} \alpha_{34}] + \alpha'_{14} c_{28} \alpha_{31} \alpha_{34} \}, \\
 A_{23}^{(l)} &= \frac{1}{\Delta_0} \{ \alpha'_{11} [c_4 \alpha_{12} \alpha_{13} + c_5 \alpha_{32} \alpha_{33} + c_6 (\alpha_{12} \alpha_{33} + \alpha_{13} \alpha_{32}) - \alpha_{12} \alpha_{43} - \alpha_{13} \alpha_{42}] - \\
 &\quad - \alpha'_{12} [c_{13} \alpha_{22} \alpha_{23} + k_{11} (\alpha_{22} \alpha_{43} + \alpha_{23} \alpha_{42})] + \alpha'_{13} [c_{16} (\alpha_{12} \alpha_{13} + \alpha_{22} \alpha_{23}) + c_{17} \alpha_{32} \alpha_{33} + c_{18} (\alpha_{12} \alpha_{23} + \alpha_{13} \alpha_{22}) + \\
 &\quad + c_{19} (\alpha_{12} \alpha_{33} + \alpha_{13} \alpha_{32}) + c_{19} (\alpha_{22} \alpha_{33} + \alpha_{23} \alpha_{32})] + \alpha'_{14} c_{28} \alpha_{32} \alpha_{33} \}, \\
 A_{24}^{(l)} &= \frac{1}{\Delta_0} \{ \alpha'_{11} [c_4 \alpha_{12} \alpha_{14} + c_5 \alpha_{32} \alpha_{34} + c_6 (\alpha_{12} \alpha_{34} + \alpha_{14} \alpha_{32})] - \alpha'_{12} k_{11} \alpha_{22} \alpha_{44} + \\
 &\quad + \alpha'_{13} [c_{16} \alpha_{12} \alpha_{14} + c_{17} \alpha_{32} \alpha_{34} + c_{18} \alpha_{14} \alpha_{22} + c_{19} (\alpha_{12} \alpha_{34} + \alpha_{14} \alpha_{32}) + c_{19} \alpha_{22} \alpha_{34}] + \alpha'_{14} c_{28} \alpha_{32} \alpha_{34} \}, \\
 A_{111}^{(1)} &= \frac{1}{\Delta_0} \{ \alpha'_{11} (c_7 \alpha_{11}^3 + c_8 \alpha_{31}^3 + 3c_9 \alpha_{11}^2 \alpha_{31}) + \alpha'_{13} [c_{21} \alpha_{31}^3 - c_{20} (\alpha_{11}^3 + \alpha_{21}^3) - 3\alpha_{11}^2 (c_{24} \alpha_{21} + c_{25} \alpha_{31}) - \\
 &\quad - 3c_{25} \alpha_{21}^2 \alpha_{31} - 6c_{26} \alpha_{31} \alpha_{11} \alpha_{21}] - \alpha'_{14} c_{29} \alpha_{31}^3 \}, \\
 A_{122}^{(1)} &= \frac{1}{\Delta_0} \{ \alpha'_{11} [c_7 \alpha_{11} \alpha_{12}^2 + c_8 \alpha_{31} \alpha_{32}^2 + c_9 \alpha_{12} (2\alpha_{11} \alpha_{32} + \alpha_{12} \alpha_{31})] + \alpha'_{13} [c_{21} \alpha_{31} \alpha_{32}^2 - c_{20} (\alpha_{11} \alpha_{12}^2 + \alpha_{21} \alpha_{22}^2) - \\
 &\quad - c_{24} \alpha_{12} (2\alpha_{11} \alpha_{22} + \alpha_{12} \alpha_{21}) - c_{25} \alpha_{12} (2\alpha_{11} \alpha_{32} + \alpha_{12} \alpha_{31}) - c_{25} \alpha_{22} (2\alpha_{21} \alpha_{32} + \alpha_{31} \alpha_{22}) - \\
 &\quad - 2c_{26} [\alpha_{32} (\alpha_{11} \alpha_{22} + \alpha_{12} \alpha_{21}) + \alpha_{12} \alpha_{22} \alpha_{31}] - \alpha'_{14} c_{29} \alpha_{31} \alpha_{32}^2 \}, \\
 A_{222}^{(2)} &= \frac{1}{\Delta_0} \{ \alpha'_{21} [c_7 \alpha_{12}^3 + c_8 \alpha_{32}^3 + c_9 \alpha_{12} \alpha_{32} (2\alpha_{12} + \alpha_{32})] + \alpha'_{23} [c_{21} \alpha_{32}^3 - c_{20} (\alpha_{12}^3 + \alpha_{22}^3) - \\
 &\quad - 3\alpha_{12}^2 (c_{24} \alpha_{22} + c_{25} \alpha_{32}) - 3\alpha_{22} \alpha_{32} (c_{25} \alpha_{22} + 2c_{26} \alpha_{12})] - \alpha'_{24} c_{29} \alpha_{32}^3 \}, \\
 A_{112}^{(2)} &= \frac{1}{\Delta_0} \{ \alpha'_{21} [c_7 \alpha_{12}^3 + c_8 \alpha_{31}^2 \alpha_{32} + c_9 \alpha_{11} (\alpha_{11} \alpha_{32} + 2\alpha_{31} \alpha_{12})] + \alpha'_{23} [c_{21} \alpha_{31}^2 \alpha_{32} - \\
 &\quad - c_{20} (\alpha_{11}^2 \alpha_{12} + \alpha_{21}^2 \alpha_{22}) - c_{24} \alpha_{11} (\alpha_{11} \alpha_{22} + 2\alpha_{21} \alpha_{12}) - c_{25} \alpha_{11} (\alpha_{11} \alpha_{32} + 2\alpha_{31} \alpha_{12}) - \\
 &\quad - c_{25} \alpha_{21} (\alpha_{21} \alpha_{32} + 2\alpha_{31} \alpha_{22}) - 2c_{26} (\alpha_{11} \alpha_{21} \alpha_{32} + \alpha_{31} (\alpha_{11} \alpha_{22} + \alpha_{12} \alpha_{21}))] - \alpha'_{24} c_{29} \alpha_{31}^2 \alpha_{32} \}.
 \end{aligned}
 \tag{A12}$$

Notice that

$$\begin{aligned}
 \alpha_{11} &= -[c_2 c_{12} c_{14} + c_3 (b^2 + c_{11} c_{15})], \alpha_{12} = bc_3 (c_{15} - c_{11}), \alpha_{21} = c_{12} (b^2 + c_2 c_{14} - c_1 c_{15}), \\
 \alpha_{22} &= -bc_{12} (c_1 + c_{15}), \alpha_{31} = c_{14} (c_1 c_{12} + c_3 c_{11}), \alpha_{32} = bc_{14} (c_{12} - c_3), \\
 \alpha_{41} &= b^2 (c_1 - c_{11} + c_{15}) - c_{11} (c_2 c_{14} - c_1 c_{15}), \alpha_{42} = b [b^2 + c_1 (c_{11} - c_{15}) + c_2 c_{14} + c_{11} c_{15}], \\
 \alpha_{23} &= -c_{12} c_{14} c_{27}, \alpha_{24} = 0, \alpha_{33} = c_{14} [(m + k_{23})(m + c_{11}) - n^2], \alpha_{44} = -nc_{14} c_{27}, \\
 \alpha_{34} &= -nc_{14} (2m + k_{23} + c_{11}), \alpha_{43} = c_{14} c_{27} (m + c_{11}), \\
 \alpha_{13} &= n^2 (c_{15} - k_{23} - c_{11} - 3m) + (m + k_{23})(m + c_{11})(m - c_{15}) + c_{12} c_{14} c_{27}, \\
 \alpha_{14} &= n [n^2 - (m + c_{11})(2m + k_{23} - c_{15}) - (m + k_{23})(m - c_{15})],
 \end{aligned}
 \tag{A13}$$

and

$$\Delta_0 = \det \begin{vmatrix} \alpha_{11} & \alpha_{12} & \alpha_{13} & \alpha_{14} \\ \alpha_{21} & \alpha_{22} & \alpha_{23} & 0 \\ \alpha_{31} & \alpha_{32} & \alpha_{33} & \alpha_{34} \\ \alpha_{41} & \alpha_{42} & \alpha_{43} & \alpha_{44} \end{vmatrix}.
 \tag{A14}$$

Using the previous formula (A14), we obtain

$$\begin{aligned}
 \alpha'_{11} &= \det \begin{vmatrix} \alpha_{22} & \alpha_{23} & 0 \\ \alpha_{32} & \alpha_{33} & \alpha_{34} \\ \alpha_{42} & \alpha_{43} & \alpha_{44} \end{vmatrix}, \alpha'_{12} = -\det \begin{vmatrix} \alpha_{12} & \alpha_{13} & \alpha_{14} \\ \alpha_{32} & \alpha_{33} & \alpha_{34} \\ \alpha_{42} & \alpha_{43} & \alpha_{44} \end{vmatrix}, \alpha'_{13} = \det \begin{vmatrix} \alpha_{12} & \alpha_{13} & \alpha_{14} \\ \alpha_{22} & \alpha_{23} & 0 \\ \alpha_{42} & \alpha_{43} & \alpha_{44} \end{vmatrix}, \\
 \alpha'_{14} &= -\det \begin{vmatrix} \alpha_{12} & \alpha_{13} & \alpha_{14} \\ \alpha_{22} & \alpha_{23} & 0 \\ \alpha_{32} & \alpha_{33} & \alpha_{34} \end{vmatrix}, \alpha'_{21} = -\det \begin{vmatrix} \alpha_{21} & \alpha_{23} & 0 \\ \alpha_{31} & \alpha_{33} & \alpha_{34} \\ \alpha_{41} & \alpha_{43} & \alpha_{44} \end{vmatrix}, \alpha'_{22} = \det \begin{vmatrix} \alpha_{11} & \alpha_{13} & \alpha_{14} \\ \alpha_{31} & \alpha_{33} & \alpha_{34} \\ \alpha_{41} & \alpha_{43} & \alpha_{44} \end{vmatrix}, \\
 \alpha'_{23} &= -\det \begin{vmatrix} \alpha_{11} & \alpha_{13} & \alpha_{14} \\ \alpha_{21} & \alpha_{23} & 0 \\ \alpha_{41} & \alpha_{43} & \alpha_{44} \end{vmatrix}, \alpha'_{24} = \det \begin{vmatrix} \alpha_{11} & \alpha_{13} & \alpha_{14} \\ \alpha_{21} & \alpha_{23} & 0 \\ \alpha_{31} & \alpha_{33} & \alpha_{34} \end{vmatrix}, \alpha'_{31} = \det \begin{vmatrix} \alpha_{21} & \alpha_{22} & 0 \\ \alpha_{31} & \alpha_{32} & \alpha_{34} \\ \alpha_{41} & \alpha_{42} & \alpha_{44} \end{vmatrix}, \\
 \alpha'_{32} &= -\det \begin{vmatrix} \alpha_{11} & \alpha_{12} & \alpha_{14} \\ \alpha_{31} & \alpha_{32} & \alpha_{34} \\ \alpha_{41} & \alpha_{42} & \alpha_{44} \end{vmatrix}, \alpha'_{33} = \det \begin{vmatrix} \alpha_{11} & \alpha_{12} & \alpha_{14} \\ \alpha_{21} & \alpha_{22} & 0 \\ \alpha_{41} & \alpha_{42} & \alpha_{44} \end{vmatrix}, \alpha'_{34} = -\det \begin{vmatrix} \alpha_{11} & \alpha_{12} & \alpha_{14} \\ \alpha_{21} & \alpha_{22} & 0 \\ \alpha_{31} & \alpha_{32} & \alpha_{34} \end{vmatrix}, \\
 \alpha'_{41} &= -\det \begin{vmatrix} \alpha_{21} & \alpha_{22} & \alpha_{23} \\ \alpha_{31} & \alpha_{32} & \alpha_{33} \\ \alpha_{41} & \alpha_{42} & \alpha_{43} \end{vmatrix}, \alpha'_{42} = \det \begin{vmatrix} \alpha_{11} & \alpha_{12} & \alpha_{13} \\ \alpha_{31} & \alpha_{32} & \alpha_{33} \\ \alpha_{41} & \alpha_{42} & \alpha_{43} \end{vmatrix}, \alpha'_{43} = -\det \begin{vmatrix} \alpha_{11} & \alpha_{12} & \alpha_{13} \\ \alpha_{21} & \alpha_{22} & \alpha_{23} \\ \alpha_{41} & \alpha_{42} & \alpha_{43} \end{vmatrix}, \\
 \alpha'_{44} &= \det \begin{vmatrix} \alpha_{11} & \alpha_{12} & \alpha_{13} \\ \alpha_{21} & \alpha_{22} & \alpha_{23} \\ \alpha_{31} & \alpha_{32} & \alpha_{33} \end{vmatrix}.
 \end{aligned}
 \tag{A15}$$

Appendix C. Qualitative Picture When Morphogen Gradients Are Equal to Zero

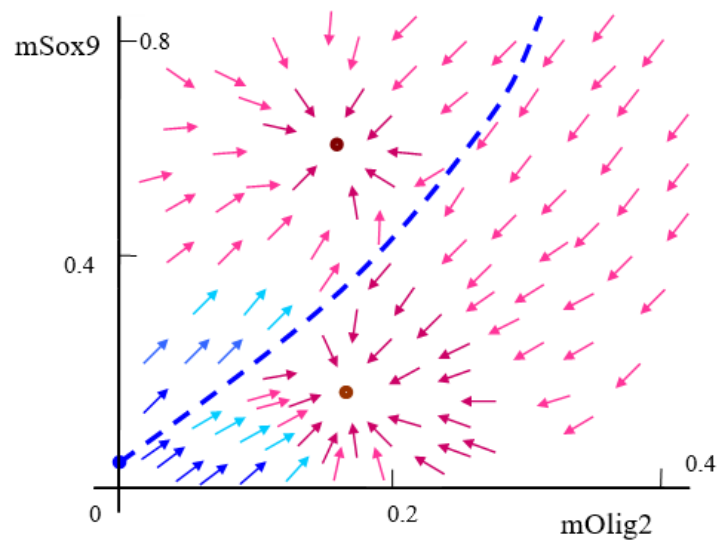


Figure A1. Sketch of the system’s bistability structure in case of $I_1 = I_2 = 0$. Dashed blue line remarks the boundary of bistability between two stable equilibria (fixed points). Red points and arrows are stable; Blue point and arrows are unstable.

Appendix D. Numerical Results for System (1) When the Bifurcation Parameters k_2 , I_1 and I_2 Have Different Values

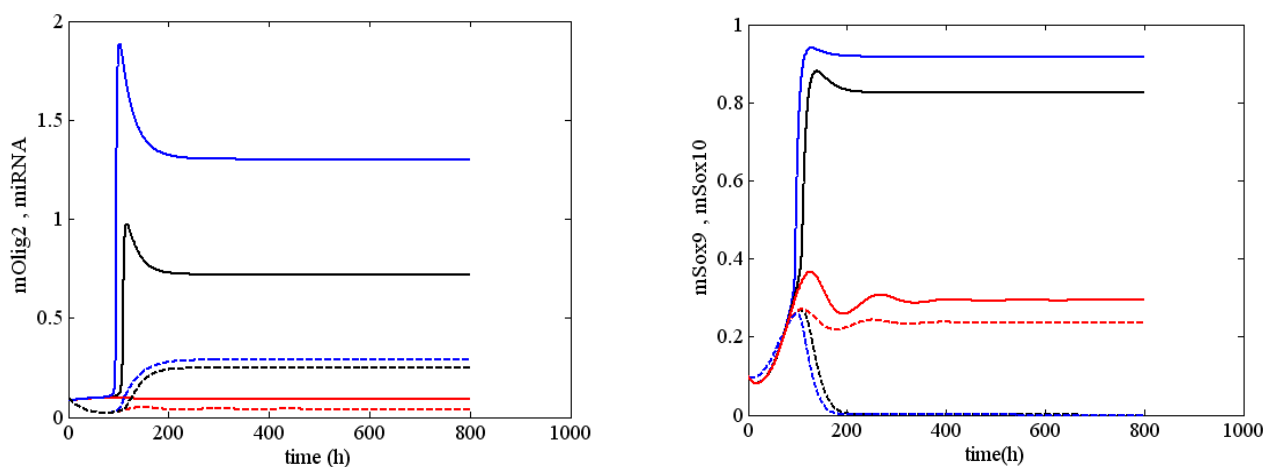


Figure A2. Various stable solutions for mOlig2 (solid line), miRNA, mSox9 and mSox10 (solid line) arising from system (1) when $I_1 = I_2 = 0$ and $k_2 = 0.4762$ (black lines); $k_2 = 0.04762$ (red line), and $k_2 = 0.95$ (blue line).

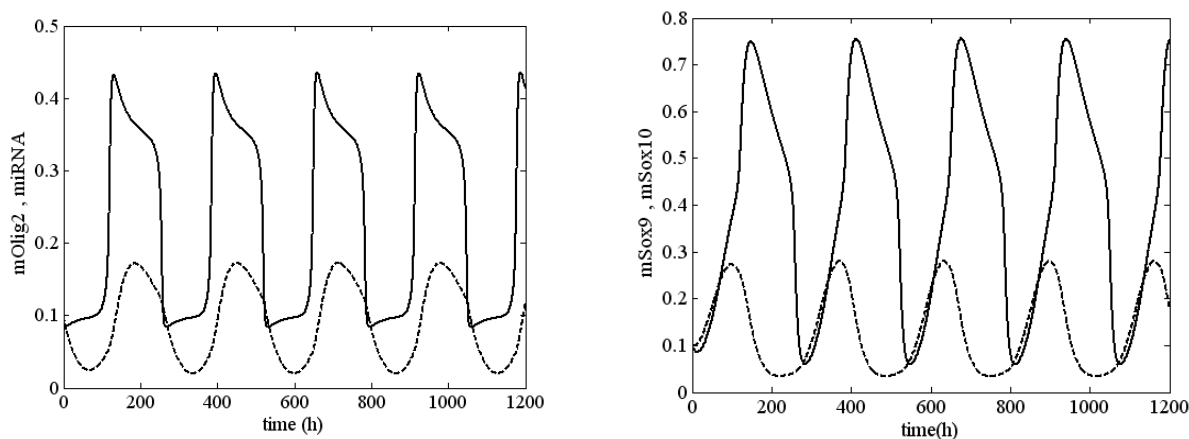


Figure A3. Periodic (sustained oscillation) solution for mOlig2 (solid line), miRNA, mSox9 and mSox10 (solid line) arising from system (1) when $I_1 = I_2 = 0.01$ and $k_2 = 0.2$. The solution for mOlig2 has a form of relaxant (fast-slow phases) oscillation.

References

1. Luo, L. *Principles of Neurobiology*, 2nd ed.; CRC Press: Boca Raton, FL, USA, 2021.
2. Waxman, S.G.; Bennett, M.V.L. Relative conduction velocities of small myelinated and non-myelinated fibres in the central nervous system. *Nat. New Biol.* **1972**, *238*, 217–219. [[CrossRef](#)]
3. Bradl, M.; Lassman, H. Oligodendrocytes: Biology and pathology. *Acta Neuropathol.* **2010**, *119*, 37–53. [[CrossRef](#)] [[PubMed](#)]
4. Kuhn, S.; Gritti, L.; Crooks, D.; Dombrowski, Y. Oligodendrocytes in development, myelin generation and beyond. *Cells* **2019**, *8*, 1424. [[CrossRef](#)] [[PubMed](#)]
5. Bergles, D.; Richardson, W. Oligodendrocyte development and plasticity. *Cold Spring Harb. Perspect. Biol.* **2016**, *8*, a020453. [[CrossRef](#)] [[PubMed](#)]
6. Santos, A.; Vieira, M.; Vasconcellos, R.; Goulart, V.; Kihara, A.; Resende, R. Decoding cell signaling and regulation of oligodendrocyte differentiation. *Semin. Cell Dev. Biol.* **2019**, *95*, 54–73. [[CrossRef](#)] [[PubMed](#)]
7. Dufour, A.; Gontran, E.; Deroulers, C.; Varlet, P.; Pallud, J.; Grammaticos, B.; Badoual, M. Modeling the dynamics of oligodendrocyte precursor cells and the genesis of gliomas. *PLOS Comput. Biol.* **2018**, *14*, e1005977. [[CrossRef](#)] [[PubMed](#)]

8. Yeung, M.S.Y.; Djelloul, M.; Steiner, E.; Bernard, S.; Salehpour, M.; Possnert, G.; Brundin, L.; Frisé, J. Dynamics of oligodendrocyte generation in multiple sclerosis. *Nature* **2019**, *556*, 538–542. [[CrossRef](#)] [[PubMed](#)]
9. Swiss, V.A.; Nguyen, T.; Dugas, J.; Ibrahim, A.; Barres, B.; Androulakis, I.P.; Casaccia, P. Identification of a Gene Regulatory Network Necessary for the Initiation of Oligodendrocyte Differentiation. *PLoS ONE* **2011**, *6*, e18088. [[CrossRef](#)] [[PubMed](#)]
10. Wittstatt, J.; Weider, M.; Wegner, M.; Reiprich, S. MicroRNA miR-204 regulates proliferation and differentiation of oligodendroglia in culture. *Glia* **2020**, *68*, 2015–2027. [[CrossRef](#)] [[PubMed](#)]
11. Wedel, M.; Fröb, F.; Elsesser, O.; Wittmann, M.-T.; Lie, D.C.; Reis, A.; Wegner, M. Transcription factor Tcf4 is the preferred heterodimerization partner for Olig2 in oligodendrocytes and required for differentiation. *Nucleic Acids Res.* **2020**, *48*, 4839–4857. [[CrossRef](#)]
12. Reiprich, S.; Cantone, M.; Weider, M.; Baroti, T.; Wittstatt, J.; Schmitt, C.; Küspert, M.; Vera, J.; Wegner, M. Transcription factor Sox10 regulates oligodendroglial Sox9 levels via microRNAs. *Glia* **2017**, *65*, 1089–1102. [[CrossRef](#)] [[PubMed](#)]
13. He, D.; Marie, C.; Zhao, C.; Kim, B.; Wang, J.; Deng, Y.; Clavairoly, A.; Frah, M.; Wang, H.; He, X.; et al. Chd7 cooperates with Sox10 and regulates the onset of CNS myelination and remyelination. *Nat. Neurosci.* **2016**, *19*, 678–689. [[CrossRef](#)] [[PubMed](#)]
14. Cantone, M.; Küspert, M.; Reiprich, S.; Lai, X.; Eberhardt, M.; Göttle, P.; Beyer, F.; Azim, K.; Küry, P.; Wegner, M.; et al. A gene regulatory architecture that controls region-independent dynamics of oligodendrocyte differentiation. *Glia* **2019**, *67*, 825–843. [[CrossRef](#)] [[PubMed](#)]
15. Aprato, J.; Sock, E.; Weider, M.; Elsesser, O.; Fröb, F.; Wegner, M. Myrf guides target gene selection of transcription factor Sox10 during oligodendroglial development. *Nucleic Acids Res.* **2020**, *48*, 1254–1270. [[CrossRef](#)]
16. Uriu, K. Genetic oscillators in development. *Dev. Growth Differ.* **2016**, *58*, 16–30. [[CrossRef](#)] [[PubMed](#)]
17. Meeuse, M.W.; Hauser, Y.P.; Morales Moya, L.J.; Hendriks, G.J.; Eglinger, J.; Bogaarts, G.; Tsiaris, C.; Großhans, H. Developmental function and state transitions of a gene expression oscillator in *Caenorhabditis elegans*. *Mol. Syst. Biol.* **2020**, *16*, e9498. [[CrossRef](#)] [[PubMed](#)]
18. Tsiaris, C.; Aulehla, A. Self-organization of embryonic genetic oscillators into spatiotemporal wave patterns. *Cell* **2016**, *164*, 656–667. [[CrossRef](#)] [[PubMed](#)]
19. Sueda, R.; Kageyama, R. Oscillatory expression of *Ascl1* in oligodendrogenesis. *Gene Expr. Patterns* **2021**, *41*, 119198. [[CrossRef](#)] [[PubMed](#)]
20. Vera, J.; Nikolov, S.; Lai, X.; Singh, A.; Wolkenhauer, O. A model-based investigation of the transcriptional activity of p53 and its feedback loop regulation via 14-3-3 σ . *IET Syst. Biol.* **2011**, *5*, 293–307. [[CrossRef](#)] [[PubMed](#)]
21. Vera, J.; Nikolov, S.; Wolkenhauer, O. Strategies to investigate signal transduction pathways with mathematical modelling. In *Systems Biology for Signalling Network*; Choi, S., Ed.; Springer: New York, NY, USA, 2010; Chapter 8; pp. 207–234.
22. Le Novère, N. The long journey to a systems biology of neuronal function. *BMC Syst. Biol.* **2007**, *1*, 28. [[CrossRef](#)] [[PubMed](#)]
23. Bullock, T.H. Have brain dynamics evolved? Should we look for unique dynamics in the sapient species? *Neural Comput.* **2003**, *15*, 2013–2027. [[CrossRef](#)]
24. Marsden, J.; McCracken, M. *The Hopf Bifurcation and its Applications*; Springer Science & Business Media: New York, NY, USA, 2012.
25. Nikolov, S.; Vera, J.; Kotev, V.; Wolkenhauer, O.; Petrov, V. Dynamic properties of a delayed protein cross talk model. *BioSystems* **2008**, *91*, 51–68. [[CrossRef](#)] [[PubMed](#)]
26. Bautin, N. *Behaviour of Dynamical Systems Near the Boundary of Stability*; Nauka: Moscow, Russia, 1984. (In Russian)
27. Shilnikov, L.P.; Shilnikov, A.L.; Turaev, D.V.; Chua, L.O. *Methods of Qualitative Theory in Nonlinear Dynamics*; World Scientific Pub Co Inc: London, UK, 1998; part I; 2001; part II.
28. Nikolov, S.; Wolkenhauer, O.; Vera, J.; Nenov, M. The role of cooperativity in a p53-miR34 dynamical mathematical model. *J. Theor. Biol.* **2020**, *495*, 110252. [[CrossRef](#)] [[PubMed](#)]
29. Shilnikov, L. Theory of bifurcation of dynamical systems and dangerous boundaries. *Dokl. Acad. Nauk.* **1975**, *224*, 1046–1049. (In Russian). [Shilnikov, L. *Math. Physics* **1975**, *20*, 674–676, (in English)]
30. Thompson, J.; Stewart, H.; Ueda, Y. Safe, explosive, and dangerous bifurcations in dissipative dynamical systems. *Phys. Rev. E* **1994**, *49*, 1019–1027. [[CrossRef](#)]
31. Bautin, N.; Shilnikov, L.L. Supplement I: Safe and dangerous boundaries of stability of stability regions. In *The Hopf-Bifurcation and its Application*; Marsden, J., McCracken, M., Eds.; Mir: Moscow, Russia, 1980.
32. Nikolov, S.; Nenov, M.; Vera, J. Investigation of a kinetic model reproducing the mechanisms of oligodendrocyte differentiation. *Ser. Biomech.* **2021**, *35*, 51–57.
33. Chicone, C. *Ordinary Differential Equations with Applications*; Springer: New York, NY, USA, 2006.
34. Smale, S. Differentiable dynamical systems. *Bull. Am. Soc.* **1967**, *73*, 747–817. [[CrossRef](#)]
35. Barres, B.A.; Lazar, M.A.; Raff, M.C. A novel role for thyroid hormone, glucocorticoids and retinoic acid in timing oligodendrocyte development. *Development* **1994**, *120*, 1097–1108. [[CrossRef](#)]
36. Nikolov, S.; Petrov, V. New results about route to chaos in Rossler system. *Int. J. Bifurc. Chaos* **2004**, *14*, 293–308. [[CrossRef](#)]
37. Andronov, A.; Witt, A.; Khaikin, S. *Theory of Oscillators: Adiwes International Series in Physics*; Elsevier: Amsterdam, The Netherlands, 2013; Volume 4.

38. Nikolov, S. First Lyapunov value and bifurcation behaviour of specific class three-dimensional systems. *Int. J. Bifurc. Chaos* **2004**, *14*, 2811–2823. [[CrossRef](#)]
39. Nikolov, S.; Vassilev, V. Dynamics of Rossler Prototype-4 System: Analytical and numerical investigation. *Mathematics* **2021**, *9*, 352. [[CrossRef](#)]
40. Nikolov, S.G.; Vassilev, V.M. Assessing the non-linear dynamics of a Hopf-Langford type system. *Mathematics* **2021**, *9*, 2340. [[CrossRef](#)]
41. Leonov, G.; Kuznetsova, O. Lyapunov quantities and limit cycles of two-dimensional dynamical systems. Analytical methods and symbolic computation. *Regul. Chaotic Dyn.* **2010**, *15*, 354–377. [[CrossRef](#)]
42. Izhikevich, E. *Dynamic Systems in Neurosciences: The Geometry of Excitability and Bursting*; The MIT Press: London, UK, 2007.